ISSN 1070-4272, Russian Journal of Applied Chemistry, 2015, Vol. 88, No. 7, pp. 1207−1218. © Pleiades Publishing, Ltd., 2015.

VARIOUS TECHNOLOGIES

Nano SiO_2-Bonded Ru-TsDPEN for Catalytic Resolution of 1,2-Propanediol by Two Transfer Hydrogenation[1]

Chuan-Jun Yue, Li-Ping Gu, Ya-Feng Zhuang, and Bao-Liang Liu

Department of Chemical Engineering, School of Science, Changzhou Institute of Technology, Changzhou, 213022 China
e-mail: czupapers@126.com

Received July 15, 2015

Abstract—A new strategy was introduced for the catalytic resolution of 1,2-propanediol involving the successive oxidative kinetic resolution and asymmetric hydrogenation by two hydrogen transfer reactions catalyzed by nano SiO_2-bonded Ru-TsDPEN [TsDPEN = *N*-(*p*-toluenesulfonyl)-1,2-diphenylethylene diamine]-derived catalysts composed of two opposite configurations. The catalysts were characterized by X-ray diffraction (XRD), transmission electron microscopy (TEM), Brunauer–Emmett–Teller (BET), Fourier-transform infrared spectroscopy (FT-IR), thermogravimetry-derivative thermogravimetry (TG-DTG) analysis, and inductively coupled plasma atomic emission spectrometry (ICP-AES). Results showed that Ru-TsDPEN derived catalysts were successfully grafted on the nano SiO_2, affording high catalytic conversions of >99 and 99%, selectivities of 47 and 98% and maximum ee values of >99 and >99% in the two reactions, which were due to the nano SiO_2 with Ru-TsDPEN in the reaction system with high dispersion. Additionally, the catalysts exhibited excellent durability and were filtered and reused at least five times without noticeable catalysts deactivations.

DOI: 10.1134/S1070427215070162

INTRODUCTION

Optically active 1,2-diols are important for preparing various materials, such as chiral medicines and natural products [1, 2]. Enantiomerically pure (*R*)-1,2-propanediol is of critical importance to the total synthesis of the anti-HIV pharmaceutical Tenofovir and related functional target molecules [3]. This class of compounds has so far been prepared using different raw materials including catalytic asymmetric dihydroxylation of olefins [4], Baker's yeast reduction of phenacyl alcohol [5], enzymatic hydrolysis of diol monoacetates [6], asymmetric hydrogenation (AH) of α-hydroxyl ketones [7], and catalytic resolution of racemic 1,2-diols consisting of kinetic [8, 9] or dynamic kinetic resolution [10]. Catalytic resolution can be improved through efficient catalysis and green 1,2-propanediol resource from the industrial hydrogenolysis of large and cheap glycerol. Glycerol is a byproduct of biodiesel production through the transesterification of biomass, and accounts for approximately 10 wt % of the converted products [11–13]. However, few studies have been conducted on the subject. Shuklov et al. [10] reported that the dynamic kinetic resolution of rac-1-*tert*- butoxypropan-2-ol with isopropenyl acetate in the presence of Novozyme 435 and a ruthenium (Ru) catalyst produces enantiomerically pure (*R*)-1-*tert*-butoxy-2-acetoxy-propane, which can be transformed into (*R*)-1,2-propanediol. Iwasaki et al. [14] developed the catalytic kinetic resolution method using a chiral organotin catalyst with benzoyl chloride. However, controversies surround the described catalytic resolution, which involves the coordination of the catalysts for the racemation and the resolution in one pot for dynamic kinetic resolution, and an intrinsic of only 50% of a desired enantiomer for kinetic resolution. Improving these methods is an urgent issue.

The AH of acetol to chiral 1,2-propanediol has been successfully performed in recent years by employing various homogeneous Ru and iridium catalysts with appropriate ligands [15–17]. Meanwhile, asymmetric

---

[1] The text was submitted by the authors in English.

Scheme 1. Schematic preparation of nano SiO_2-bonded Ru-TsDPEN derived catalysts.

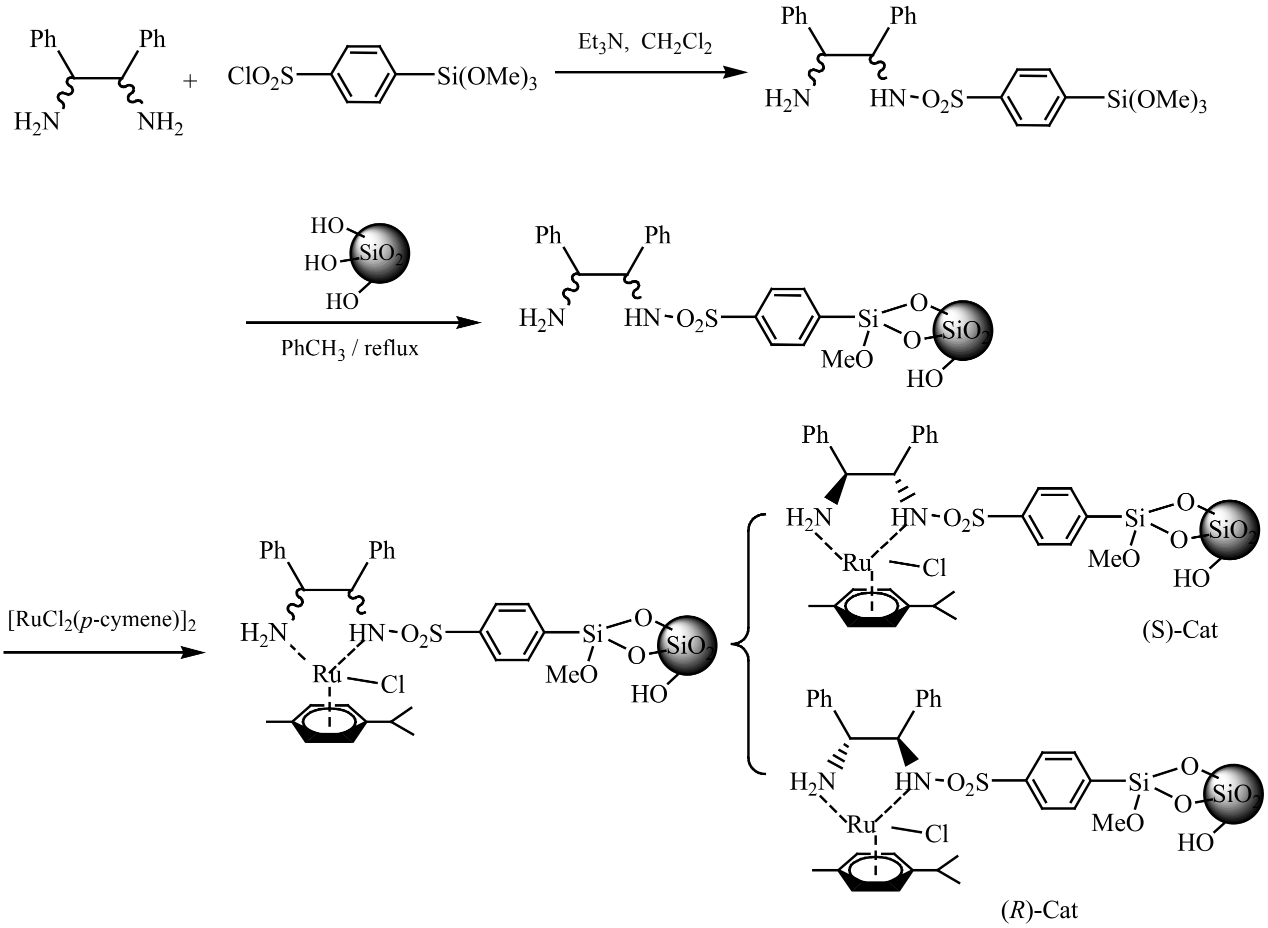

transfer hydrogenation (ATH) with reversible property has also received considerable attention because of its high-quality performance, operational simplicity, and the availability of reductants [18]. Among the various chiral catalysts reported, more attention has been paid to Ru-based catalysts, especially Ru-*N*-(*p*-toluenesulfonyl)-1,2-diphenylethyl-enediamine (Ru-TsDPEN) catalysts developed by Noyori et al. [19]. These catalysts have been widely applied to reduce prochiral ketones via AH and ATH, which show excellent enantioselectivities in propan-2-ol [20, 21]. Although metal complex-based AH and ATH were proven reliable, catalytic transformations for green chemistry focus on high efficiency, low cost, easy separation, and minimal waste. Catalysts that can be easily separated and recyclable through filtration are preferable, providing easy operation and clean transformation from laboratory to large-scale production. Several catalysts on insoluble supports have been reported for AH and ATH [22–26]. However, their heterogenized catalyst recovery through filtration or centrifugation remains problematic, and their catalytic efficacy is unsatisfactory because catalytically active species tends deactivate during handling. Additionally, the acetol as a starting material is unstable for synthetic chiral 1,2-propanediol. New methods must be explored to avoid these drawbacks.

An oxidation kinetic resolution by ATH that combines AH of oxidized byproduct is introduced. This process involves the successive performance of the oxidation kinetic resolution of 1,2-propanediol and the AH of acetol by nano SiO_2-supported Ru-TsDPEN catalysts with opposite configuration, respectively. The desired product configuration may be obtained by the regulated ligand configuration sequence. The strategy potentially allows the adaptation of the immobilized catalysts to the successive flow processes. The present study mainly investigated the preparation of nano SiO_2-supported Ru-TsDPEN and their properties as well as their physical characterization and the completely catalytic resolution of 1,2-propanediol through successive two opposite configuration catalyst to (*R*)- or (*S*)-1,2-propanediol.

EXPERIMENTAL

General. $[RuCl_2(p\text{-cymene})]_2$ was purchased from Zhejiang Metallurgical Research Institute Co., Ltd. (1*R*,2*R*)-DPEN and (1*S*,2*S*)-DPEN, triethylamine, 2-(4-chlorosulfonylphenyl)ethyltrimethoxysilane, nano SiO_2 (15 ± 5 nm), toluene, isopropaneol, acetone, 1,2-propanol, acetol, CH_3OH, and CH_2Cl_2 were obtained from Aladdin. (*R*)-propanediol was obtained from Acros.

CH_2Cl_2 and CH_3OH were distilled from CaH_2 and Mg/I_2, respectively. Toluene was freshly distilled from a deep-blue solution of sodium-benzophenone under nitrogen. Triethylamine was distilled and stored away from light. Nano SiO_2 was heated at 150°C for 3 h and cooled in nitrogen before use. Other reagents and chemicals were degassed thrice under a nitrogen atmosphere, and used without further purification.

Catalyst preparation. The nano SiO_2-bonded Ru-TsDPEN derived catalysts were prepared according to Scheme 1.

The catalysts were synthesized according to the analog method described in the literature [27, 28].

Synthesis of modified TsDPEN ligand. (1*R*, 2*R*)- or (1*S*, 2*S*)-DPEN (0.318 g, 1.5 mmol) was dissolved in 15 mL of CH_2Cl_2 with 0.3 mL of triethylamine, a solution of 2-(4-chlorosulfonylphenyl)ethyltrimethoxysilane (0.38 g, 1.12 mmol) in 15 mL CH_2Cl_2 was then added dropwise at 0°C in 50 mL flasks. After the dropping was completed, the mixture was slowly warmed to room temperature and unceasingly stirred for 4 h, then the solvent was removed in vacuo. The residue subsequently fast passed through a 15 cm silica gel column (eluent: $Et_3N : CH_3OH : CH_2Cl_2 = 1 : 10 : 100$), concentrated, and dried in vacuo to obtain 90.5% yield of modified DPEN. ^1H NMR (400 MHz, $CDCl_3$): 1.95 (s, 2H), 2.03 (s, 1H), 3.56 (s, 9H), 4.32 (d, $J = 5.3$ Hz, 1H), 4.51 (d, $J = 5.3$ Hz, 1H), 7.02–7.41 (m, 14H). IR (KBr): 3352, 3295, 3170, 3061, 3027, 2942, 2840, 1901, 1690, 1603, 1494, 1453, 1411, 1342, 1266, 1192, 1153, 1089, and 1014 cm^{-1}.

Preparation of nano SiO_2-bonded modified TsDPEN. The predried nano SiO_2 (1.5 g) and the synthesized ligand (0.13 g) were added to 20 mL of dry toluene in 50 mL flasks. The mixture was refluxed for 24 h in nitrogen. After filtration, the obtained white solid was successively washed with 30 mL toluene and 50 mL solvent mixture of CH_2Cl_2 and CH_3OH (1 : 1). The solid was then suspended in 20 mL mixture solvent and stirred overnight. After filtration and thorough washing with 25 mL solvent mixture and 25 mL CH_3OH the wet solid was dried at 55°C in vacuo for 24 h to afford the immobilized ligand. IR (KBr tablet): 3441, 2962, 1640, 1503, 1460, 109, 802, 703, 560, and 467 cm^{-1}.

Preparation of nano SiO_2-bonded Ru-TsDPEN derived catalysts. $[RuCl_2(p\text{-cymene})]_2$ (0.33g, 0.53 mmol), nano SiO_2-bonded (1*R*,2*R*)- or (1*S*,2*S*)-TsDPEN (0.39 g, 1.07 mmol), and triethylamine (0.3 mL, 2.15 mmol) in 12 mL 2-propanol were stirred at 85°C for 1.5 h. The gray solid was collected by filtration and washed with a little of deoxygenated water. After washing in a Soxhlet extraction in methanol overnight, the solid was dried in vacuo to obtain the loaded Ru catalyst, ICP-AES analysis showed that 70.5% yield was achieved from Ru content, and element analysis of the bonded complex calculated from mass percentage of N demonstrated that loading ratio of the TsDPEN ligand was 2.45 mmol g^{-1}. Catalysts were denoted as (*S*)-Cat and (*R*)-Cat according to the different configurations, using $[Ru]/SiO_2$ as a representation.

Catalyst characterization. ^1H NMR spectra were recorded on a Bruker Avance-400 (400 MHz) spectrometer, chemical shifts are expressed in parts per million downfield from TMS at $\delta = 0$ ppm, and J values were given in Hz. ICP-AES was performed on a PerkinElmer ICP/6500 ICP spectrometer. Nitrogen element analysis was carried out on EA2400 elemental analyzer (Perkin Elmer). XRD patterns were recorded on Rigaku D/Max 2500 PC X-ray diffractometer, treated with CuK_a radiation over the 2θ range of 10°–80°. Specific surface areas were measured by N_2 adsorption/desorption by the BET method on a Micromeritics Autochem 2910 analyzer. The samples were degassed for 10 h at 100°C before the measurement. TEM micrographs were acquired using a JEOL JEM-1230 transmission electron microscope. Sample thermostabilities were determined on PerkinElmer's Pyris 1 TGA device (Setsys 170 Thermogravimetric Analyzer, Setaram, France). The experiments were performed under N_2 atmosphere from room temperature to 500°C at a ramp rate of 5°C min^{-1}. FT-IR spectra were performed on IR200 (Thermo Fisher) spectrometer from 400 cm^{-1} to 4000 cm^{-1}.

Scheme 2. The (*S*)- and (*R*)-Ru-TsDPEN/SiO_2 catalytic two hydrogen transfer reaction of oxidative kinetic and asymmetric hydrogenation.

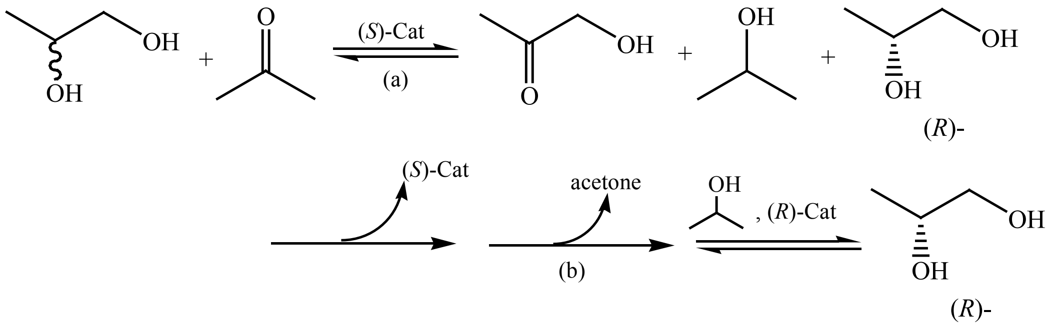

Catalytic kinetic resolution of 1,2-propanediol. The catalytic resolution of 1,2-propanediol involved two reactions by hydrogen transfer. The first step (a) was the catalytically oxidative kinetic resolution of 1,2-propanediol, and the second step (b) was the catalytically AH of acetol (Scheme 2).

In the catalytically oxidized kinetic resolution and AH of acetol, all reactions were conducted under a nitrogen atmosphere using analogous Schlenk-type techniques. Typically, 0.5 mg (*S*)-Cat, 28 mL acetone, 0.56 mg KOH in 10 mL water, and 7 mL 1,2-propanediol were orderly added into 100 mL flasks, and the mixture was stirred at 40°C for 20 h. After the reaction, the catalyst was filtered from the mixture, and 5 μL filtrate was extracted by syringe for further gas chromatography (GC) analysis. Other liquids were separated by miniature vacuum distillation from the solution of acetone and water. The remainder liquid, containing (*R*)-1,2-propanediol and acetol, was introduced into the step (b) reaction. The liquid, as substrate, and a supplemental 5 mL isopropaneol and 10 mL 5.6 g L^{-1} KOH aqueous solution were orderly placed in 100 mL flasks. The mixture was degassed thrice, and 0.5 mg (*R*)-Cat was added. The reaction system was stirred while being heated to 40°C until reaction completion. The workup of step (b) was conducted by the analogous method of step (a). Obtained samples were analyzed by GC (GC4011A chromatograph equipped with a flame ionization detector and CP-Chirasil-Dex CB capillary column), and 1-butaneol was added as internal standard. Product quality was assessed on a GC-MS spectrometer (GCQ, Thermo Finnigan). The collected (*R*)- and (*S*)-Cat were tested for the next run without further modification. Substrate conversions, selectivity (chiral product in each reation), yield, and ee (chiral product) value were calculated by the following equations:

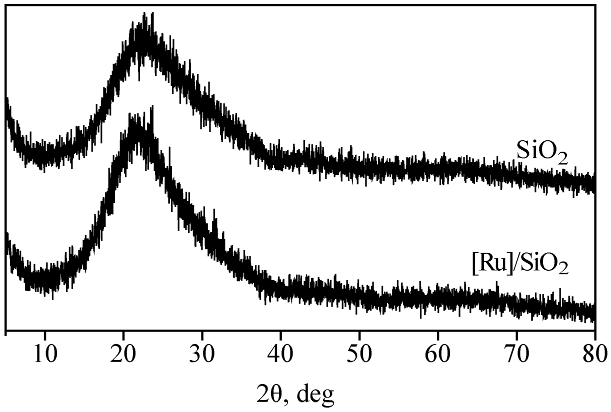

Fig. 1. XRD pattern of nano SiO_2 and [Ru]/SiO_2.

Conversion (%) = [(initial mass of reactive material – mass of none-reactive material)/initial mass of reactive material] × 100%.

Selectivity (%) = (all (*R*)-1,2-propanediol product mass in the reaction system/all products mass) × 100%.

$$\text{ee}\ (\%) = [|(R) - (S)|/(R) + (S)]$$

(*R*- or *S*-configuration contained all the same compound in the reaction system).

RESULTS AND DISCUSSION

Catalysts properties. (*S*)- and (*R*)-[Ru]/SiO_2 catalysts, featuring the same presentation, were characterized as follows.

Wide-angle XRD. Nano SiO_2 is selected as parent support because of its large surface area and sizable pore volume, which can suitably accommodate bulky catalysts comfortably, facilitate substrate diffusion, and

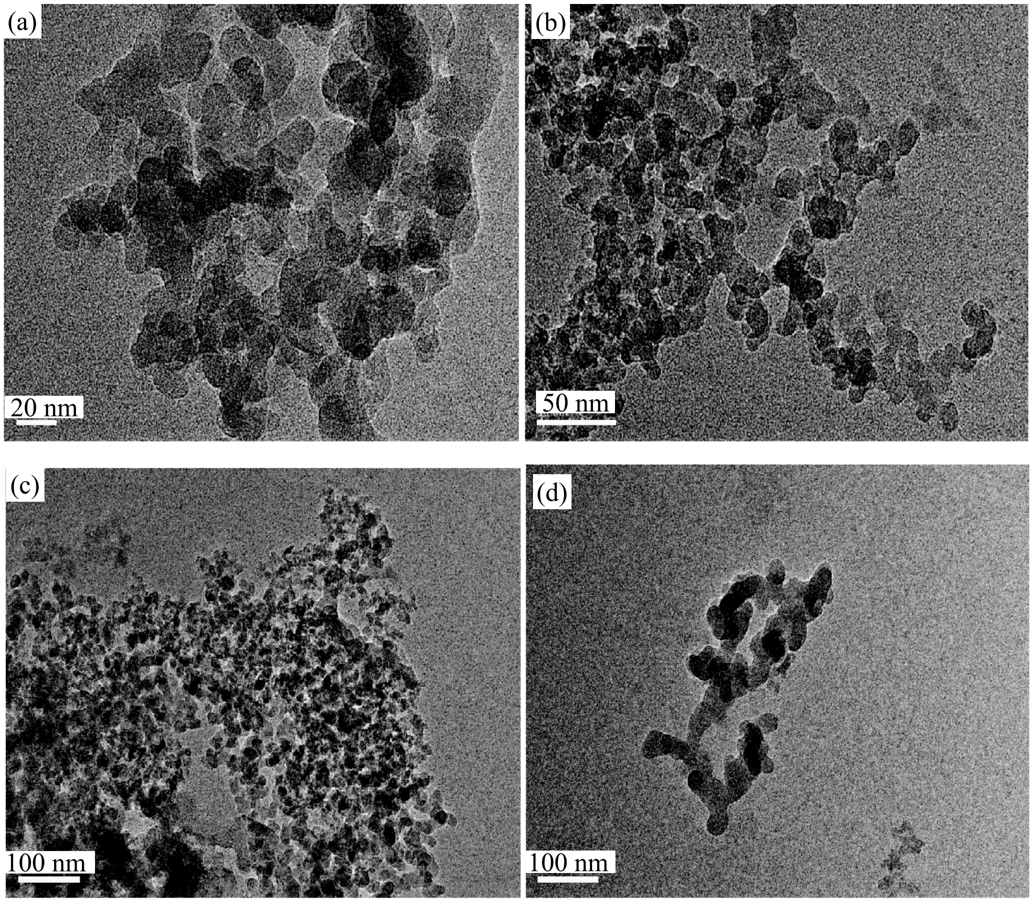

Fig. 2. The TEM images of $[Ru]/SiO_2$. (a), (b) Ordered nano SiO_2 texture with micro cluster. (c), (d) [Ru] complex at the transition position between dense dark shadow to light gray.

effectively disperse in some solvents. The modified DPEN ligand by trimethoxysilyl was grafted onto the surface of the nano SiO_2 (Scheme 1). Subsequently, nano SiO_2 with TsDPEN-derived ligand reacted with $[RuCl_2$ (*p*-cymene)$]_2$. The wide-angle XRD patterns of the nano SiO_2 and supported Ru-TsDPEN catalyst are shown in Fig. 1. Only one typical peak for the nano SiO_2 parent was observed in the 2θ angle of 22.5°, and the large peak width could be attributed to finer nanosized particles compared with ordinary silica gel [29]. Average nanoparticles size was approximately 15.1 nm as calculated by Debye–Scherrer equation based on the (111) crystal plane. No obvious change was present after subsequent surface modification. The nano SiO_2 surface modification did not result in nano SiO_2 particle alteration. However, the peak shape of the modified nano SiO_2 became narrow, indicating that successful graft leads to larger nanoparticles.

TEM analysis. The transmission electron micrograph in Fig. 2 shows the morphological structure of $[Ru]/SiO_2$. In Figs. 2a and 2b, the background with cross mapping and enhanced brightness and shading clearly show general ordered nano SiO_2 texture existing in the micro cluster in a small range. Figure 2c shows the [Ru] catalyst and nano SiO_2 interlaced image, which imply that the [Ru] catalyst is grafted on nano SiO_2. The transition site from the dense dark shadow to light gray is attracted to the [Ru] catalyst. Figure 2d demonstrates that the [Ru] catalyst perspective with enhanced dispersion was showed clearly due to the changed surface nature of nano SiO_2 after the the SiO_2-supported [Ru] catalyst to reduce the interaction of nano SiO_2 surface, demonstrating that the [Ru] catalyst grafted on nano SiO_2 was not evenly dispersed. The mean particle size of nano SiO_2 with the [Ru] catalyst was approximately 15.2 nm based on the statistical analysis of the transmission electron micrographs of $[Ru]/SiO_2$. Contrary to [30], nanosilica

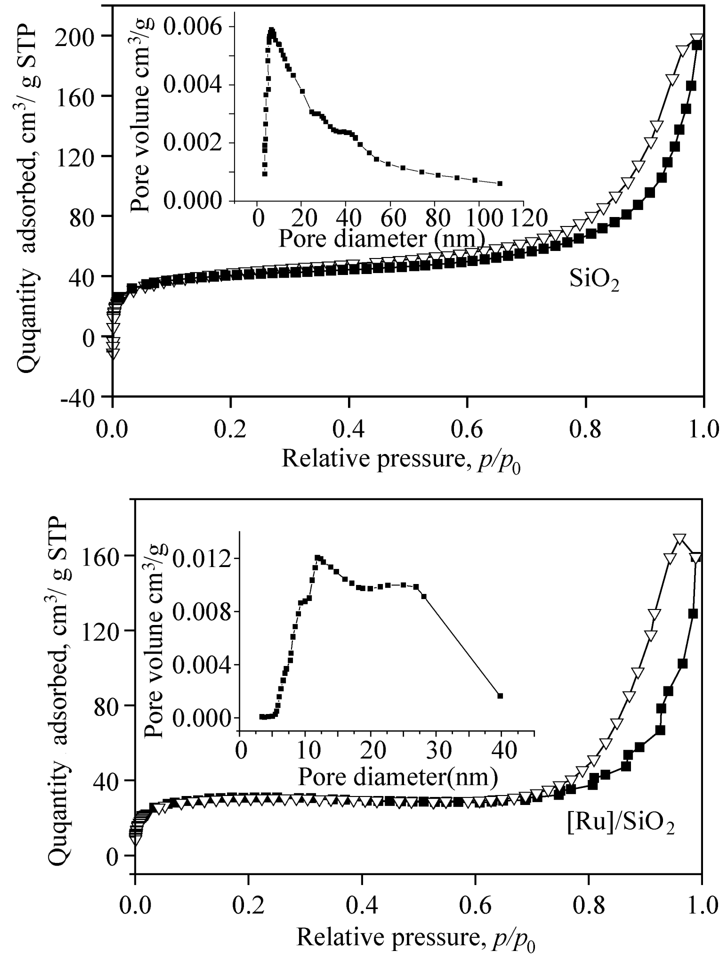

Fig. 3. Nitrogen adsorption-desorption isotherms of nano SiO_2 and $[Ru]/SiO_2$.

improved catalyst dispersion.

N_2 sorption study. Textural properties of nano SiO_2 and $[Ru]/SiO_2$ were detected by N_2 sorption experiment. Both catalysts have analog IV type adsorption isotherms typical of mesoporous features, but derived from the accumulation holes of nano SiO_2, which is not mesoporous (Fig. 3). Pore diameter distribution obviously differed between nano SiO_2 and $[Ru]/SiO_2$. The latter had a bigger pore diameter because the enhanced volume of [Ru]-loaded SiO_2 enlarged the particle diameter. The textural of specific surface areas, pore size, and pore volume of nano SiO_2 and $[Ru]/SiO_2$ catalysts are reported in Table 1. The corresponding BET surface areas were 129.2 and 90.5 $m^2 g^{-1}$, Langmuir surface areas were 195.8 and 132.1 $m^2 g^{-1}$, average pore volumes were 0.25 and 0.23 $cm^3 g^{-1}$, and average pore sizes were 16.4 and 16.1 nm. Although $[Ru]/SiO_2$ values were consistently lower than the parent nano SiO_2, the N_2 sorption isotherm pattern of the former was of typical type IV pattern (Fig. 3), similar to that of nano SiO_2. The texture structure of nano SiO_2 did not remarkably accumulate after grafting of [Ru] catalyst, consistent with the transmission electron micrograph. Thus, the [Ru] catalyst was successfully grafted on the nano SiO_2 surface.

FT-IR spectroscopy. Comparative results of the IR spectra of nano SiO_2 and $[Ru]/SiO_2$ (Fig. 4), the latter displays some new bands at 2927.4, 2856.1, 1993.1, 1492.1, 1839.8, and 668.2 cm^{-1}. The bands at 1839.8 and 1993.1 cm^{-1} are assigned to the S=O and S–C vibrations. The bands at 1492.1 cm^{-1} is attributed to the C=C vibration of phenyl group. The bands at 2927.4 and 2856.1 cm^{-1} are assigned to the alkyl chain C–H stretching vibration. The bands at 668.2 cm^{-1} are

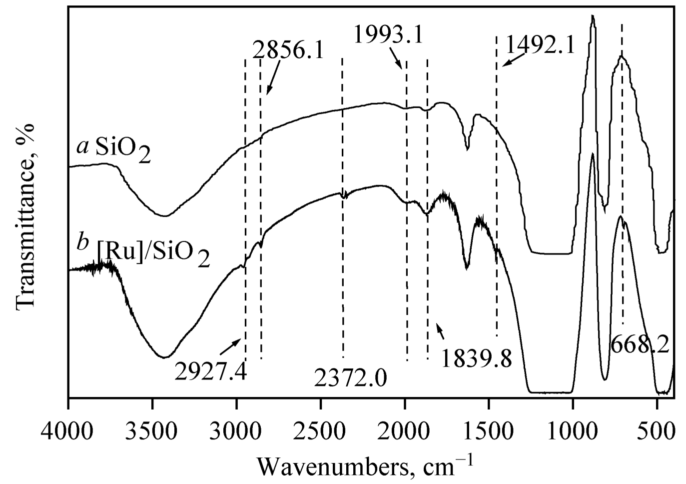

Fig. 4. The FTIR spectra of nano SiO_2 and [Ru]/SiO_2.

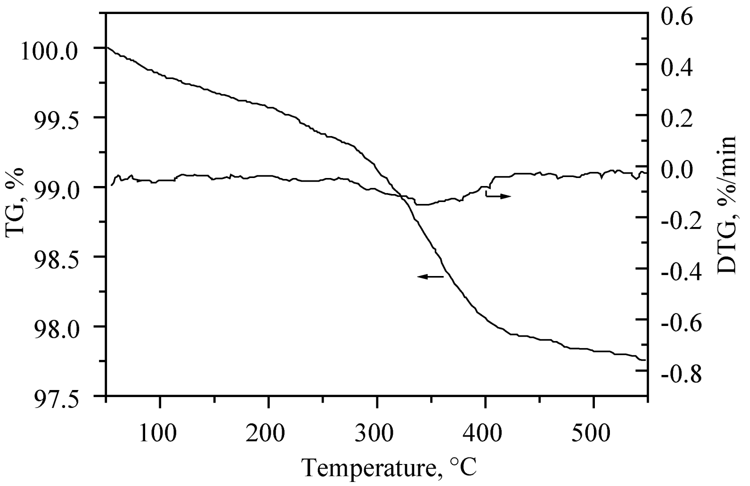

Fig. 5. The TG-DTG curves of [Ru]/SiO_2.

Table 1. Texture parameters of nano SiO_2 and [Ru]/SiO_2

Sample	Specific surface area, $m^2 g^{-1}$		Average pore volume, $cm^3 g^{-1}$	Average pore diameter, nm
	BET	Langmuir		
Nano SiO_2	129.2	195.8	0.25	16.4
[Ru]/SiO_2	90.5	132.1	0.23	16.1

Table 2. The tentative results of catalytic non-interfering substrates by [Ru]/SiO_2 catalysts via hydrogen transfer[a]

Reaction step	Catalyst	Substrate	Conversion, %	Selectivity, %	ee, %
(a)	(*S*)-Cat	PD/acetone	88	47	75
(b)	(*R*)-Cat	(*R*)-PD/acetol/propan-2-ol	95	98	>99

[a] Reaction conditions: (a) catalysts 0.5 mg, PD 7 mL, PD/acetone 0.25 (V/V), KOH 0.56 mg (in 10 mL water), *T* 40°C, *t* 20 h; (b) catalysts 0.5 mg, acetol 8 mL, acetol/isopropaneol 025(V/V), KOH 0.56 mg (in 10 mL water), *T* 40°C, *t* 15 h.

Table 3. Effect of feeding sequence on the catalytic resolution of 1,2-propanediol[a]

Reaction step	Feeding sequence	Conversion, %	Selectivity, %	ee, %
(a)	Substrate → Catalyst → KOH (aq)	85	47	74
	Substrate → KOH(aq) → Catalyst	89	48	79
	Catalyst → KOH(aq) → Substrate	80	46	67
(b)	Substrate → Catalyst → KOH (aq)	96	98	98
	Substrate → KOH(aq) → Catalyst	96	98	98
	Catalyst → KOH(aq) → Substrate	95	98	97

[a] Reaction conditions: (a) catalysts 0.5 mg, PD 7 mL, PD/acetone 0.25 (V/V), KOH 0.56 mg (in 10 mL water), $T = 40$°C, $t = 20$ h. (b) Catalysts 0.5 mg, acetol 8 mL, acetol/isopropaneol 025(V/V), KOH 0.56 mg (in 10 mL water), $T = 40$°C, $t = 15$ h.

Table 4. Effect of substrates ratio on the catalytic resolution of 1,2-propanediol[a]

Reaction step	Substrates ratio, mol		Conversion, %	Selectivity, %	ee, %
(a)	Acetone/PD	0.5	47	42	30
		1.0	59	46	41
		2.0	82	46	70
		4.0	98	47	96
		6.0	>99	41	89
(b)	Propan-2-ol/ acetol	0.5	35	92	99
		1.0	51	92	>99
		2.0	79	95	>99
		4.0	>99	98	>99
		6.0	>99	97	>99

[a] Reaction conditions: (a) catalysts 0.5 mg, PD 7 mL, KOH 0.56 mg (in 10 mL water), T 40°C, $t = 20$ h .(b) Catalysts 0.5 mg, acetol 8 mL, KOH 0.56 mg (in 10 mL water), $T = 40$°C, $t = 15$ h.

assigned to the breathing vibration of phenyl ring. Even though the nano SiO_2 partly covers the IR absorption peak of [Ru] complex [25], results combining the element analysis, presenting the 2 : 1 molar ratio of nitrogen and Ru in the [Ru]/SiO_2 further confirm a successful grafting of [Ru] on nano SiO_2.

Thermoanalysis. Catalysts thermostability is reflected further by TG-DTG profile. The [Ru]/SiO_2 catalysts exhibited a total weight loss of approximately 2.28% from room temperature to 600°C (Fig. 5). From room temperature to close to 300°C, the DTG profile was almost parallel, which could be attributed to the even release of physical adsorption water. Stronger thermogravimetric change between 300 and 400°C could be assigned to the oxidation decomposition of Ru-TsDPEN molecule [31], probably containing the dehydration from silicon hydroxyl condensation, resulting in approximately 1.3% of weight loss. Above 400°C, weight loss is mainly because of silicon hydroxyl dehydration. The almost parallel DTG curve shows that during temperature increase, SiO_2 showed no obvious aggregation, because the particle aggregation should be accompanied with significant DTG progress caused by the close relation of surface change and energy with thermal gravity. The catalyst is thermostable in the catalytic reaction temperature.

Feasibility of the successively catalytic hydrogen transfer for 1,2-propanediol resolution. The substrate with two hydroxyl or functional carbonyl can perform hydrogen transfer reactions of kinetic resolution and AH in Ru-DPEN catalysts [32, 33]. However, total yields are inherently not more than 50% in catalytically kinetic resolution, and dynamic kinetic resolution has lower catalytic efficacy because of the difficulty in catalyst coordination in one pot. Therefore, the catalytic oxidation kinetic resolution of 1,2-propanediol and asymmetric hydrogenation of acetol from the previous reaction as a by-product was conducted to improve the utilization of raw materials and catalytic efficacy. The feasibility of the two step reactions was verified using synthesized (*S*)-Cat and (*R*)-Cat on independent 1,2-propanediol/acetone and (*R*)-propanediol/acetol/propan-2-ol substrate systems for catalytic hydrogen transfer reaction, respectively. Table 2 shows that the feasibility of the catalytic resolution of 1,2-propanediol by two step reactions, and the corresponding catalytic conversions reached 88% and 95%, and the corresponding selectivity for (*R*)-1,2-propanediol and ee values were 47 and 98%, and 75 and >99%, respectively. This may be understood from the characteristics of the reversible reactions and the products composition (Scheme 2). GC-MS results showed that the introduction of the catalytic by-products from the first step including the oxidized product of primary alcohols in 1,2-propanediol and its condensation with acetone, resulted in decreased conversion to the desired product except for the reaction equilibrium, and relatively low ee value was presumed that it derived from the indistinctive rate difference in hydrogen transfer from (*S*)- and (*R*)-propanediol to acetone. Additionally, (*S*)-1,2-propanediol was achieved when the order of catalyst feeding was changed, that is, (*R*)-Cat was used in the first reaction and (*S*)-Cat in the second. The industrial production of desired chiral products was convenient.

Catalytic kinetic resolution of 1,2-propanediol. The synthesized $[Ru]/SiO_2$ catalysts were tested in the successive oxidative kinetic resolution of 1,2-propanediol and AH of acetol to evaluate its effectiveness as well as to determine the effects of reaction parameters. Some of the parameters, such as solvent and alkali, were optimized [34, 35], which was significant to the effects of the reaction on the feeding sequence, substrate ratio, and temperature.

Effect of feeding sequence on catalytic resolution. Table 3 demonstrates the effect of feeding sequence on the substrate, KOH, and catalyst on two catalytic reactions. Substrate → KOH(aq) → catalyst sequence values (89% conversion, 48% selectivity to (*R*)-1,2-propanediol and 79% ee) in the catalytic oxidative kinetic resolution were higher than those of substrate → catalyst → KOH(aq) order (85% conversion, 47% selectivity and 74% ee), and without the order based on the catalyst → KOH (aq) → substrate process (80% conversion 46% selectivity and 67% ee) (Table 3) in the catalytic oxidative kinetic resolution. This is explained by more effectively generated Ruthenium hydride active species in the way of substrate → KOH(aq) → catalyst because of the active species being introduced on the premise of the hydroxyl and KOH reaction to alcohol-alkali [18]. Although the catalytic results in the second sequence is not closely related to the feeding sequence, with over 95% conversion and ee as reported in the literature [36], propan-2-ol is an outstanding hydrogen donor for the hydrogen transfer system.

Effect of substrates ratio on the catalytic resolution. Substrates ratio affects the reversible reaction equilibrium involved in conversion and ee. The effect of substrates molar ratio was examined. Table 4 shows that the conversions increased with molar ratio of acetone to 1,2-propanediol and propan-2-ol to acetol in the same way of from 1 : 2 to 6 : 1 on the two catalytic reactions, with maximum >99% and >99% conversions, respectively. For ee, when acetone/1,2-propanediol ratio exceeded 4 with 96% ee, stereoselectivity began to decrease to 89% at a ratio of 6 because the excessive acetone promoted the 1,2-propanediol to transform other products, including organic oxides such as 2-hydroxy propionic aldehyde and condensation compounds such as 2,2,4-trimethyl-1,3-dioxolane, based on GC-MS results. The ee value was relatively stable (above 99%) in the catalytic AH. The change of catalytical selectivity to (*R*)-1,2-propanediol is not obvious in two step reactions, which indicates that the directional performance of the catalysts is excellent.

Effect of temperature on the catalytic resolution. Temperature is another basic parameter that affects the thermodynamic equilibrium of a reaction, activity, and enantioselectivity of the [Ru]-catalyzed chiral resolution. For the two reactions, the effect on both reaction conversion and enantioselectivity was tested from 10 to 50°C , as previously reported [34].

As is shown in Table 5, the increase in conversion with increasing temperature is expected and with the usual value, that is, >99% conversions both at 50°C in the catalytic oxidative kinetic resolution and at 40°C in the second reaction. And the selectivity of two step reactions decreases with an temperature increase due to the overmuch byproducts. By contrast, ee values increased as temperature rose from 10 to 40°C in the first reaction and from $10^{\circ C}$ to 30°C in the second. As

Table 5. Effect of temperature on the catalytic resolution of 1,2-propanediol[a]

Reaction step	Temperature, °C	Conversion, %	Selectivity, %	e.e., %
(a)	10	69	49	51
	20	71	49	53
	30	89	49	78
	40	96	47	96
	50	>99	44	88
(b)	10	60	99	>99
	20	81	99	>99
	30	>99	98	>99
	40	>99	98	>99
	50	>99	95	97

[a] Reaction conditions: (a) catalysts 0.5 mg, PD 7 mL, PD/acetone 0.25 (V/V), KOH 0.56 mg (in 10 mL water), $T = 40$°C, $t = 20$ h. (b) Catalysts 0.5 mg, acetol 8 mL, acetol/isopropaneol 025 (V/V), KOH 0.56 mg (in 10 mL water), $t = 15$ h.

Table 6. Reusability of the nano SiO_2-supported Ru-TsDPEN derived catalysts for successive oxidative kinetic resolution and asymmetric hydrogenation[a]

Recycle runs		1	2	3	4	5
Conversion, %	(a)	96	96	96	95	93
	(b)	>99	96	91	88	85
Selectivity, %	(a)	47	47	47	47	46
	(b)	98	97	97	96	94
ee, %	(a)	99	99	99	98	98
	(b)	>99	99	98	92	89

[a] Reaction conditions: (a) catalysts 0.5 mg, PD 7 mL, PD/acetone 0.25 (V/V), KOH 0.56 mg (in 10 mL water), $T = 40$°C, $t = 20$ h .(b) catalysts 0.5 mg, acetol 8 mL, acetol/isopropaneol 025 (V/V), KOH 0.56 mg (in 10 mL water), $T = 40$°C, $t = 15$ h.

temperature rose above 40 and 30°C in the two reactions, ee value dropped, showing that catalyst conformation may not be well recognized with reaction substrates in the catalytic system at high temperatures [37], resulting in decreasing enantioselectivity. The corresponding maximum ee values of (*R*)-1,2-propanediol were 96% and >99%, respectively.

Catalysts recyclability and stability. The recyclability of [Ru]/SiO_2 was tested under optimized conditions. The catalysts were collected by filtration, acetone was removed by distillation after the first reaction, and propan-2-ol was added by syringe before the second. Table 6 demonstrates the better recycling of the catalysts. [Ru]/SiO_2 can be consecutively reused for at least five times with conversion ranging from >99% to 93% in the first reaction and form >99% to 85% in the second, and the selectivity decrease from 47 to 46%, and 98 to 94%, whereas corresponding ee valve changed from 99 to 98%, and >99 to 89%, respectively. Decrease in catalytic activity was mainly due to catalyst loss caused by the handling process, derived from the destroyed and irreparable active species of ruthenium hydride. The 9.1 mol % Ru from ICP analysis leached from the catalyst after five runs. The decrease in ee value also implies that the catalyst decomposed partly in consecutive reuses, which indicates an ineffective coordination of some TsDPEN ligand and Ru.

Catalyst stability is closely related to the catalyst nature and specific catalytic mechanism. Generally, Ru-TsDPEN catalyst for hydrogen transfer between the hydroxyl and carbonyl is of a bifunctional synergistic catalytic process involving $-NH_2$ ligand and metal

Ru, and energy calculation for the transition state [40] illustrated that propan-2-ol as hydrogen donor is favorable to the reaction. This finding is also supported by various studies [39, 40]. Catalytic ATH of acetol was smoothly conducted. Catalytically asymmetric hydrogen transfer between 1,2-propanediol and acetone was difficult, with relatively harsh reaction conditions, because the reaction needs to be successively performed after ruthenium hydride is generated and effective electron energy state matching among substrates and catalyst occurs. Ru-TsPDEN may exert the best life in a successive flow environment considering its excellent performance in hydrogen transfer reaction catalysis.

CONCLUSIONS

A new strategy was developed for the resolution of 1,2-propanediol by successive oxidative kinetic resolution and AH catalyzed by the opposite configuration Ru-TsDPEN/nano-SiO_2 via hydrogen transfer. The configuration of the product was controlled by changing the sequence of using two opposite configuration catalysts. The heterogeneous catalysts showed excellent activities and enatioselectivities for two hydrogen transfer with considerable recovery and reuse by simple filtration. The catalysts were reused consecutively for at least five times without noticeable loss of conversion and ee values. This study provides a potential and general approach for secondary alcohol resolution. The system has great potential for industrial application if catalyst stability can be further enhanced.

ACKNOWLEDGMENTS

We thank Nature Science Foundation of Jiangsu Province (Grant No BK2011235) for financial support.

REFERENCES

1. Gupta, P., Naidu, S.V., and Kumar, P., *Tetrahedron Lett.,* 2004, vol. 45, pp. 849–851.
2. Yoshikawa, N., Xu, F., Arredondo, J.D., and Itoh, T., *Org. Process Res. Dev.,* 2011, vol. 15, pp. 824–830.
3. Barral, K., Priet, S., Sire, J., Neyts, J., Balzarini, J., Canard, B., and Alvarez, K., *J. Med. Chem.,* 2006, vol. 49, pp. 7799–7806.
4. Dehury, S.K., Hariharakrishnan, V.S., *Tetrahedron Lett.,* 2007, vol. 48, pp. 2493–2496.
5. Bálint, J., Egri, G., Kolbert, A., Dianóczky, C., Fogassy, E., Novák, L., and Poppe, L., *Tetrahedron: Asymmetry,* 1999, vol. 10, pp. 4017–4028.
6. Poppe, L., Novák, L., Kajtár-Peredy, M., and Szántay, C., *Tetrahedron: Asymmetry,* 1993, vol. 4, pp. 2211–2217.
7. Busygin, I., Taskinen, A., Nieminen, V., Toukoniitty, E., Stillger, T., Leino, R., and Murzin, D.Y., *J. Am. Chem. Soc.,* 2009, vol. 131, pp. 4449–4462.
8. Petursson, S. and Jonsdottir, S., *Tetrahedron: Asymmetry,* 2011, vol. 22, pp. 1809–1812.
9. Edin, M., Martín-Matute, B., and Bäckvall, J-E., *Tetrahedron: Asymmetry,* 2006, vol. 17, pp. 708–715.
10. Shuklov, I.A., Dubrovina, N.V., Schulze, J., Tietz, W., and Börner, A., *Tetrahedron Lett.,* 2014, vol. 55, pp. 3495–3497.
11. Montes, V., Checa, M., Marinas, A., Boutonnet, M., Marinas, J.M., Urbano, F.J., Järas, S., and Pinel, C., *Catal. Today,* 2014, vol. 223, pp. 129–137.
12. Yue, C.J., Gu, L.P., Su, Y., and Zhu, S.P., *Reac. Kinet. Mech. Cat.,* 2014, vol. 111, pp. 633–645.
13. Jiménez-Morales, I. , Vila, F. , Mariscal, R., and Jiménez-López, A., *Appl.Catal. B,* 2012, vols. 117, vol. 118, pp. 253–259.
14. Iwasaki, F., Maki, T., Nakashima, W., Onomura, O., and Matsumura, Y., *Org.Lett.,* 1999, vol. 1, pp. 969–972.
15. Kadyrov, R., Koenigs, R.M., Brinkmann, C., Voigtlaender, D., and Rueping, M., *Angew. Chem. Int. Ed.,* 2009, vol. 48, pp. 7556 –7559.
16. Xu, H., Meng, Q.H., and Zhang, Z.G., *Chin. J. Chem.,* 2008, vol. 26, pp. 1656–1658.
17. Ohkuma, T., Utsumi, N., Watanabe, M., Tsutsumi, K., Arai, N., and Murata, K., *Org. Lett.,* 2007, vol. 9, pp. 2565–2567.
18. Ikariya, T. and Blacker, A.J., *Acc.Chem.Res.,* 2007, vol. 40, pp. 1300–1308.
19. Fujii, A., Hashiguchi, S., Uematsu, N., Ikariya, T.., and Noyori, R., *J.Am.Chem.Soc.,* 1996, vol. 118, pp. 2521–2567.
20. Faller, J.W. and Lavoie, A.R., *Org. Lett.,* 2001, vol. 3, pp. 3703–3706.
21. Patti, A. and Pedotti, S., *Tetrahedron: Asymmetry,* 2010, vol. 21, pp. 2631–2637.
22. Shi, J. , Li, X. , Wang, Q.R. , Zhang, Y.H ,. And Tang, Y., *J. Catal.,* 2012, vol. 291, pp. 87–94.
23. Sahoo, S., Kumar, P., Lefebvre, F., and Halligudi, S.B., *Appl.Catal., A,* 2009, vol. 354, pp. 17–25.
24. Mihalcik, D.J., and Lin, W.B., *Angew. Chem. Int. Ed.,* 2008, vol. 47, pp. 6229–6232.

25. Im, J-S., Ahn, S-H., and Park, Y-H., *Chem. Eng. J.,* 2013, vol. 234, pp. 49–56.
26. Li, J., Zhang, Y.M., Han, D.F., Gao, Q., and Li, C., *J. Mol. Catal. A, Chem.,* 2009, vol. 298, pp. 31–35.
27. Liu, P.N., Gu, P.M., Wang, F., and Tu, Y.Q., *Org. Lett.,* 2004, vol. 6, pp. 169–172.
28. Ikariya, T., Hashiguchi, S., Murata, K., and Noyori, R., *Organic Syntheses,* 2005, vol. 82, pp. 10–17.
29. Mukharjee, B.B. and Barai, S.V., *Construction and Building Materials,* 2014, vol. 68, pp. 416–425.
30. Liu, P.N., Gu, P.M., Deng, J.G., Tu, Y.Q., and Ma, Y.P., *Eur. J. Org. Chem.,* 2005, vol. 15, pp. 3221–3227.
31. Liu, R., Cheng, T.Y., Kong, L.Y., Chen, C., Liu, G.H., and Li, H.X., *J. Catal.,* 2013, vol. 307, pp. 55–61.
32. Caro, Y., Torrado, M., Masaguer, C.F., and Raviña, E., *Tetrahedron: Asymmetry,* 2003, vol. 14, pp. 3689–3696.
33. Ros, A., Magriz, A., Dietrich, H., Lassaletta, J.M., and Feŕnandez, R., *Tetrahedron,* 2007, vol. 63, pp. 7532–7537.
34. Zhang, J.N., Yang, X.R., Zhou, H., Li, Y.Y., Dong, Z.R., and Gao, J.X., *Green Chem.,* 2012, vol. 14, pp. 1289–1292.
35. Han, M.L., Hu, X.P., Huang, J.D., Chen, L.G., and Zheng, Z., *Tetrahedron: Asymmetry,* 2011, vol. 22, pp. 222– 225.
36. Koike, T., Murata, K., and Ikariya, T., *Org.Lett.* 2000, vol. 2, pp. 3833–3836.
37. Pecháek, J., Václavik, J., Prech, J., Šot, P., Janušcak, J., Vilhanova, B., Vavrik, J., Kuzma, M., and Kacer, P., *Tetrahedron: Asymmetry,* 2013, vol. 24, pp. 233–239.
38. Comas-Vives, A., Ujaque, G., and Lledós, A., *THEOCHEM* 2009, vol. 903, pp. 123–132.
39. Chelucci, G., *Coord. Chem. Rev.,* 2013, vol. 257, pp. 1887–1932.
40. Clavero, P., Grabulosa, A., Font-Bardia, M., Muller, G., *J. Mol. Catal. A: Chem.,* 2014, vol. 391, pp. 183–190.